

# Analysis of natural killer–cell function in familial hemophagocytic lymphohistiocytosis (FHL): defective CD107a surface expression heralds Munc13-4 defect and discriminates between genetic subtypes of the disease

Stefania Marcenaro, Federico Gallo, Stefania Martini, Alessandra Santoro, Gillian M. Griffiths, Maurizio Aricó, Lorenzo Moretta, and Daniela Pende

**Natural killer (NK) cells from patients with familial hemophagocytic lymphohistiocytosis because of *PRF1* (FHL2, n = 5) or *MUNC13-4* (FHL3, n = 8) mutations were cultured in IL-2 prior to their use in various functional assays. Here, we report on the surface CD107a expression as a novel rapid tool for identification of patients with Munc13-4 defect. On target interaction and degranulation, FHL3 NK cells displayed low levels of surface CD107a staining, in contrast to healthy control**

**subjects or perforin-deficient NK cells. B-EBV cell lines and dendritic cell targets reveal the FHL3 NK-cell defect, whereas highly susceptible tumor targets were partially lysed by FHL3 NK cells expressing only trace amounts of Munc13-4 protein. Perforin-deficient NK cells were completely devoid of any ability to lyse target cells. Cytokine production induced by mAb-crosslinking of triggering receptors was comparable in patients and healthy control subjects. However, when cyto-**

**kine production was induced by coculture with 721.221 B-EBV cells, FHL NK cells resulted in high producers, whereas control cells were almost ineffective. This could reflect survival versus elimination of B-EBV cells (ie, the source of NK-cell stimulation) in patients versus healthy control subjects, thus mimicking the pathophysiologic scenario of FHL. (Blood. 2006;108:2316-2323)**

© 2006 by The American Society of Hematology

## Introduction

Hemophagocytic lymphohistiocytosis (HLH) is a rare, heterogeneous fatal disease of early infancy characterized by a hyperinflammatory syndrome with fever, hepatosplenomegaly, cytopenia, hypertriglyceridemia, hypofibrinogenemia, and, in some cases, central nervous system alteration. Histologic examination of involved organs (more commonly bone marrow aspiration) typically shows infiltration of lymphocytes and histiocytes with hemophagocytosis.<sup>1-3</sup> Characteristic findings are also the high levels of various cytokines, such as interleukin 6 (IL-6), IL-8, IL-10, IL-18, interferon  $\gamma$  (IFN- $\gamma$ ), and tumor necrosis factor  $\alpha$  (TNF- $\alpha$ ) and also high plasma concentrations of sCD25 and sCD95-ligand.<sup>4-6</sup> In some cases HLH may occur in patients of any age undergoing therapeutic immune suppression. In such cases, also defined as “secondary,” immune suppressive treatment withdrawal may result in control of HLH.<sup>7</sup> The remaining (also called “primary”) forms are of genetic origin and often defined as familial hemophagocytic lymphohistiocytosis (FHL). A genetic heterogeneity underlies FHL. The most common genetic defects in patients with FHL involve the perforin gene (*PRF1*) on chromosome 10q21 and the *MUNC13-4* gene on chromosome 17q25.<sup>8,9</sup> Mutations of *PRF1* account for approximately 30% to 40% of patients, defined as FHL2 subtype, and

*MUNC13-4* mutations are identified in an additional 25% to 30% of cases (FHL3). The proteins encoded by both genes are implicated in the killing machinery.<sup>10</sup> Very recently, mutations in the syntaxin11 gene (6q24) have been reported in a small group of patients (FHL4) with common Kurdish origin.<sup>11</sup> This defect is thought to alter intracellular vesicle trafficking of the phagocytic system.

*PRF1* gene encodes perforin as an inactive precursor form, which, after processing in a post-Golgi apparatus by proteolysis and glycosylation, becomes an active protein.<sup>12</sup> This mature form of perforin is stored with granzymes in specialized secretory lysosomes, known as lytic granules, which are present in natural killer (NK) and cytotoxic T lymphocytes (CTLs).<sup>13</sup> On target-cell interaction, lytic granules polarize and release their content at the immunologic synapse.<sup>14</sup> The secreted perforin then inserts into the lipid bilayer and following polymerization generates poly-perforin pores in the plasma membrane of target cells.<sup>15</sup> This pore formation leads to the destruction of cells by osmotic lysis and by allowing entry of apoptosis-inducing granzymes.<sup>16</sup> Munc13-4, a member of Munc13 family of proteins involved in vesicle priming function, has been described as a positive regulator of secretory lysosome exocytosis.<sup>9</sup> Although

From the Istituto Giannina Gaslini, Genoa, Italy; the Sir William Dunn School of Pathology, Oxford, United Kingdom; the Istituto Nazionale per la Ricerca sul Cancro, Genoa, Italy; the Onco Ematologia Pediatrica, Ospedale dei Bambini “G. Di Cristina,” Palermo, Italy; Dipartimento di Medicina Sperimentale (DIMES), University of Genoa, Italy; and the Centro di Eccellenza per la Ricerca Biomedica, University of Genoa, Italy.

Submitted April 10, 2006; accepted May 30, 2006. Prepublished online as *Blood* First Edition Paper, June 15, 2006; DOI 10.1182/blood-2006-04-015693.

Supported by grants from the Associazione Italiana per la Ricerca sul Cancro (AIRC; L.M., D.P., A.S., and M.A.); the Istituto Superiore di Sanità (ISS; L.M. and D.P.); the Ministero della Salute (L.M., D.P., M.A., and A.S.); the Associazione per la Ricerca sulle Sindromi Emofagocitiche-Istiocitosis (ARSE)

(M.A.); the Ministero dell’Istruzione dell’Università e della Ricerca (MIUR), the Fondazione Compagnia di San Paolo, the European Union FP6, and grant LSHB-CT-2004-503 319-Allostem (L.M. and D.P.); the Wellcome Trust, United Kingdom (G.M.G. and F.G.); and by a fellowship from the Fondazione Italiana per la Ricerca sul Cancro (FIRC; S.M.).

**Reprints:** Daniela Pende, Istituto Nazionale per la Ricerca sul Cancro, L.go R. Benzi 10, 16132 Genova, Italy; e-mail: daniela.pende@istge.it.

The publication costs of this article were defrayed in part by page charge payment. Therefore, and solely to indicate this fact, this article is hereby marked “advertisement” in accordance with 18 U.S.C. section 1734.

© 2006 by The American Society of Hematology

Munc13-1 functions as a priming factor in neural cells, Munc13-4 is highly expressed in several hematopoietic cells. In patients with FHL3, Munc13-4 deficiency results in defective cytolytic granule exocytosis, despite polarization of the lytic granules and docking with the plasma membrane.<sup>9</sup> Recent evidence shows that Munc13-4 binds to Rab27A; the 2 proteins colocalize on the membranes of secretory lysosomes in CTL and mast cells and promote the dense core granule secretion in platelets.<sup>17,18</sup> Rab27A is highly expressed in melanocytes and hematopoietic and other secretory cells. Absence of functional Rab27A causes the Griscelli syndrome type 2, a genetic disorder characterized by defects of pigmentation and of granule exocytosis in CTLs, in which lytic granules fail to dock on the plasma membrane and therefore do not release their content.<sup>19</sup> Thus, these fatal genetic disorders which display similar pathologic and clinical features all disrupt the release or function of cytotoxic proteins.

Defects in cellular cytotoxicity, excessive production of inflammatory cytokines, and abnormal macrophage activation characterize HLH.<sup>20</sup> In these patients an impairment of cytolytic activity of NK cells, that provide the first line of host defense, and subsequently of CTL, results in a markedly reduced ability to control viral infection. Uncontrolled viral dissemination together with a parallel excessive inflammatory reaction results in extensive tissue damage. Two major mechanisms of cytotoxicity are perforin/granzyme- and death receptor (eg, FasL and TRAIL)-mediated pathways.<sup>21,22</sup> Many studies, including experiments with perforin-deficient mice, led to the conclusion that NK cells primarily use the perforin/granzyme pathway to eliminate virus-infected or transformed cells.<sup>22</sup> Function of NK cells is regulated by an array of different receptors.<sup>23-25</sup> Human NK cells are equipped with activating receptors (ie, the NCRs NKp46, NKp30 and NKp44, NKG2D, DNAM-1) and coreceptors (ie, 2B4, NKp80, NTBA, and CD59) that once engaged by the specific ligands on target cells induce their lysis.<sup>26-30</sup> The function of activating receptors is under the control of inhibitory NK receptors, namely KIRs (CD158), which recognize shared allelic determinants of classic HLA-A, -B, or -C, and the CD94/NKG2A heterodimeric receptor, which interacts with HLA-E.<sup>31-34</sup> The general concept is that MHC class I-deficient aberrant cells are susceptible to NK-mediated lysis, whereas normal cells are protected from NK cells by the expression of HLA class I molecules.<sup>35</sup> However, among normal cells an exception is represented by immature dendritic cells (iDCs), which are characterized by low amounts of surface HLA class I molecules, particularly HLA-E, which render them highly susceptible to lysis by autologous NK cells.<sup>36</sup> In contrast, mDCs, expressing higher levels of HLA class I molecules, are protected from NK cytotoxicity in an autologous setting. Importantly, NK cells are capable of negatively selecting those DCs that did not acquire the capability of optimal Ag presentation and T-cell priming.<sup>37-40</sup> It is of note that, in response to virus-infected or tumor-transformed cells, NK cells also release cytokines and chemokines which can activate or recruit multiple cell types, thus contributing to the inflammatory response.<sup>41,42</sup>

Differential diagnosis of HLH may be difficult.<sup>43</sup> The presence of a family history of HLH-like episodes, or consanguinity, may induce the suspicion of a genetic defect underlying HLH. Yet analysis of genetic mutations is not widely accessible, because of being time consuming and expensive. Recently, cytofluorimetric analysis of perforin expression became available,<sup>44</sup> whereas rapid screening of FHL3 has not been reported so far.

In the present study, we characterized the functional patterns of NK cells derived from patients with the 2 most frequent subtypes of

FHL (FHL2 and FHL3). Our data also provide a novel tool for rapid identification of patients with FHL3 and discrimination between genetic defects.

## Patients, materials, and methods

### Patients

This study was approved by the institutional review board at the Istituto G. Gaslini. Peripheral blood samples were obtained from patients with HLH, diagnosed following current diagnostic criteria,<sup>2,3</sup> after informed consent according to the Declaration of Helsinki. Five patients with FHL2 were included in this study, and the mutations in the *PRF1* gene are listed in Table 1. Eight patients with FHL3 with *MUNC13-4* gene mutations are described in Table 2. Main clinical features of these patients are summarized in Table 3. All patients were treated according to the HLH-94 protocol.<sup>45</sup>

### *PRF1* and *MUNC13-4* gene sequencing

Sequences of *PRF1* and *MUNC13-4* genes were retrieved from the National Center for Biotechnology Information (NCBI). To analyze *PRF1* and *MUNC13-4* genes, exons and adjacent intronic regions were amplified, from genomic DNA, and directly sequenced in both directions (BigDye Terminator Cycle Sequencing Ready Reaction Kit; Applied Biosystems, Foster City, CA). Sequence primers used for amplification are available on request. Sequences obtained by ABI PRISM 3130 Sequence Detection System (Applied Biosystem) were analyzed and compared with the reported gene structure using the dedicated software SeqScape (Applied Biosystem).

### Monoclonal antibodies and cytofluorimetric analysis

The following mAbs, produced in our laboratory, were used in this study: JT3A (IgG2a, anti-CD3), c127 (IgG1, anti-CD16), c218 (IgG1, anti-CD56), BAB281 and KL247 (IgG1 and IgM, respectively, anti-NKp46), Z231 and KS38 (IgG1 and IgM, respectively, anti-NKp44), A76 and F252 (IgG1 and IgM, respectively, anti-NKp30), BAT221 (IgG1, anti-NKG2D), MAR206 (IgG1, anti-CD2), PP35 (IgG1, anti-2B4), and A6-136 (IgM, anti-HLA class I).<sup>27,29,46</sup> Anti-CD56-PC5 (N901, IgG1 mAb; Beckman Coulter, Marseille, France), anti-CD3-FITC (HIT3, IgG2a; BD Pharmingen, San Diego, CA), and anti-CD107a-PE (H4A3, IgG1; BD Pharmingen) were also used. Antibody concentrations were adjusted according to the protocol of the manufacturer. Surface phenotype of NK cells was assessed by indirect immunofluorescence using the appropriate mAb followed by PE-conjugated isotype-specific goat anti-mouse second reagent (Southern Biotechnology, Birmingham, AL). For perforin detection intracytoplasmic staining of NK cells was performed using cytofix/cytoperm (BD

**Table 1. Perforin mutations in patients with FHL2**

UPN, mutations	Mutation type	Predicted effect
<b>210</b>		
del 50T	Homozygous	L17 FsX
<b>235</b>		
del 847-852	Heterozygous	del L283-L284
C272T	Heterozygous	A91V
<b>256</b>		
C272T	Heterozygous	A91V
G695A	Heterozygous	R232H
<b>314</b>		
G1122A	Homozygous	W374X
<b>306</b>		
G1122A	Heterozygous	W374X
C657A	Heterozygous	Y219X

Perforin gene mutations in both alleles are listed in the table, including 5 patients with FHL. Perforin expression was tested by flow cytometry, and was found to be absent in all 5 patients.

UPN indicates unique patient number; X, stop; Fs, frameshift.

**Table 2. *MUNC13-4* mutations in patients with FHL3**

UPN, mutations	Mutation type	Predicted effect	Munc13-4 expression
<b>180</b>			Absent
G175A	Heterozygous	A59T	
753 + 1G > T	Homozygous	splice error	
<b>277</b>			Trace
del 3082C	Heterozygous	1028 Fs	
G1241T, C2782T	Heterozygous	R414L, R928C	
<b>249</b>			Trace
A1847G	Homozygous	E616G	
<b>237</b>			Trace
A1847G	Heterozygous	E616G	
G1241T, C2782T	Heterozygous	R414L, R928C	
<b>225</b>			Trace
A1847G	Heterozygous	E616G	
753 + 1G > T	Heterozygous	splice error	
<b>289</b>			Trace
A610G, C2650T	Heterozygous	M204V, Q884X	
ins G3226	Heterozygous	1076 FsX	
<b>293</b>			Reduced
del 1822-1833	Homozygous	del V608-A611	
<b>336</b>			Absent
G175A	Homozygous	A59T	
del 441A	Homozygous	147 Fs	

*MUNC13-4* gene mutations in both alleles are listed in the table, including 8 patients with FHL. Munc13-4 expression was tested by Western blot.

UPN indicates unique patient number; X, stop; Fs, frameshift.

Pharminggen) and labeling with either anti-perforin-PE ( $\delta$ G9, IgG2b; Ancell, Bayport, MN) or a PE-conjugated isotype matched control as previously described.<sup>47</sup>

Flow cytometric analysis was performed by FACS (FACSCalibur cytometer (BD Pharmingen)).

### Isolation and culture of NK-cell populations

NK cells from healthy donors and patients with FHL were purified using the RosetteSep method (StemCell Technologies, Vancouver, BC, Canada). Briefly, 5 to 10  $\times 10^6$  peripheral blood mononuclear cells (PBMCs) mixed with autologous red blood cells (RBCs) (RBC/PBMC ratio of 30:1) were resuspended in 1 mL 10% FCS-RPMI and were incubated with 50  $\mu$ L RosetteSep cocktail for 20 minutes at room temperature. The sample, diluted 2 times with medium, was layered on Ficoll-Hypaque gradients and centrifuged. Highly purified NK cells were recovered at the interface with optimal efficiency. NK cells were cultured on irradiated feeder cells in the presence of 2  $\mu$ g/mL phytohemagglutinin (Sigma-Aldrich, Irvine, United Kingdom) and 100 U/mL rIL-2 (Proleukin; Chiron, Emeryville, CA) to obtain proliferation and great expansions of polyclonal NK-cell populations.

### Cytolytic assay

Polyclonal NK-cell populations were tested in a 4-hour <sup>51</sup>Cr-release assay for cytolytic activity against the erythroleukemia K562, the HLA-class I<sup>-</sup> melanoma FO-1, the HLA-class I<sup>-</sup> B-EBV cell line 721.221 (thereafter termed 221), and the HLA-class I<sup>+</sup> B-EBV cell line AMALA. We also used iDCs, derived from healthy individuals as previously described,<sup>36</sup> as target cells. Masking of HLA-class I molecules was accomplished with the addition of saturating amounts of A6-136 mAb. For redirected killing assays, the murine mastocytoma Fc $\gamma$ Rc<sup>+</sup> P815 cell line was used as a target cell in the presence of mAbs specific to triggering receptors of IgG isotype at a concentration of 0.5  $\mu$ g/mL. The E/T ratios are indicated in the text.

### CD107a assay

We performed the degranulation assay quantifying cell surface CD107a expression, as previously described with minor modifications.<sup>48</sup> Briefly, 2  $\times 10^5$  polyclonal NK-cell populations or 24 hour IL-2-activated PBMCs were cocultured with 2  $\times 10^5$  target cells (K562, FO-1, 221, or P815 cells) in 96 V-bottom well plates. In each well, containing 200  $\mu$ L E/T cell suspension, 5  $\mu$ L PE-conjugated anti-CD107a mAb (BD Pharmingen) were added prior to incubation. Cells were mixed by gentle pipetting and incubated for 2 hours at 37°C in 5% CO<sub>2</sub>. To induce r-ADCC against P815, NK cells were incubated with 50  $\mu$ L IgG1 mAbs as indicated in the text. Thereafter, the cells were collected, washed in PBS, and stained with anti-CD3-FITC and anti-CD56-PC5 mAbs for flow cytometric analysis (FACSCalibur; Becton Dickinson). Surface expression of CD107a was assessed in the CD56<sup>+</sup> cell fraction of either CD3<sup>-</sup> PBMC or polyclonal NK-cell populations.

### NK-cell stimulation and cytokine analysis

Polyclonal NK-cell populations from patients and healthy donors were stimulated as follows. NK cells (1.5  $\times 10^5$ /well) were cultured overnight in 96-well flat-bottom plastic plates (200  $\mu$ L/well) precoated or not with the anti-NKp30 mAb (F252, 10  $\mu$ g/mL), the anti-NKp46 mAb (KL247, 10  $\mu$ g/mL), the anti-NKp44 (KS38, 10  $\mu$ g/mL), anti-CD16 (c127, 1  $\mu$ g/mL), or anti-CD56 as control mAb (A6/220, 10  $\mu$ g/mL). NK cells (1.5  $\times 10^5$ /well) were also stimulated by overnight coculture with 221 B-EBV cell line (5  $\times 10^4$ /well) in U-bottom plastic plates (200  $\mu$ L/well). The culture supernatants were then collected and analyzed for the presence of TNF- $\alpha$  and IFN- $\gamma$ . Cytokine analysis was carried out using enzyme-linked immunosorbent assay (ELISA) kits from Bio-Source International (Camarillo, CA) according to the manufacturer's instructions.

### Immunoblotting

Polyclonal activated NK cells were washed in PBS and lysed at 2  $\times 10^7$  cells/mL in 50 mM Tris [tris(hydroxymethyl)aminomethane] HCl [pH 8], 150 mM NaCl, 1 mM MgCl<sub>2</sub>, 1% Triton X-100 with complete protease inhibitor (Roche Diagnostics, Lewes, United Kingdom) for 15 minutes on ice, vortexing every 5 minutes. Nuclei and membranes were spun at

**Table 3. Main characteristics of patients with FHL**

Characteristic	Patients with FHL2, UPN					Patients with FHL3, UPN							
	210	235	256	314	306	180	225	237	249	277	289	293	336
Age at diagnosis, mo	2	3	60	2	4	2	144	84	96	108	3	2	4
Sex	M	F	M	F	F	F	F	M	F	M	M	F	M
Fever	+	+	+	+	+	+	+	+	+	+	+	-	+
Splenomegaly	+	+	+	+	+	+	+	+	+	+	+	+	+
Cytopenia	+	+	+	+	+	+	+	+	+	+	+	+	+
Hypertriglyceridemia	ND	+	+	+	+	+	+	ND	-	+	-	+	+
Hypofibrinogenemia	+	-	+	+	+	+	-	+	-	+	+	+	+
HSCT	Y	Y	N	Y	Y	N	N	Y	Y	Y	N	Y	Y
Outcome	DoD	Alive	Alive	DoD	Alive	DoD	DoT	Alive	Alive	Alive	DoD	Alive	Alive

UPN indicates unique patient number; HSCT, allogeneic hematopoietic stem cell transplantation; +, present; -, absent; ND, not determined; DoD, dead of disease; and DoT, dead of toxicity.

16 000g for 15 minutes at 4°C. Lysates were resolved by SDS gel electrophoresis (SDS-PAGE) on NuPAGE 4% to 12% Bis-Tris gels (Invitrogen, Paisley, United Kingdom) under reducing conditions. Proteins were transferred to nitrocellulose membranes (Invitrogen) using an XCellIII blot module (Invitrogen) in 25 mM Tris (pH 8.3), 192 mM glycine, and 20% methanol. Membranes were blocked in PBS, 5% milk powder, and 0.1% Tween20 for 1 hour at room temperature, incubated overnight at 4°C with rabbit anti-Munc13-4 antibody raised against amino acids 1 to 262 (a gift from Hisanori Horiuchi).<sup>18</sup> Membranes were washed 3 times in PBS/0.1% Tween20 for 10 minutes each and incubated for 1 hour with HRP-labeled anti-rabbit Ig secondary antibody (Jackson ImmunoResearch Laboratories, West Grove, PA) diluted in blocking buffer. Excess HRP was removed by washing 3 times in PBS/0.1% Tween20 for 10 minutes each and developed for 5 minutes in Supersignal (Perbio Science UK, Cramlington, United Kingdom), exposed for 1 minute to 1 hour using Biomax Film (Kodak, Sigma-Aldrich). SeeBlue Plus2 (Invitrogen) was loaded on each gel as molecular weight standards. The membranes were normalized using a rabbit antiactin antibody (Sigma-Aldrich).

### Immunofluorescence microscopy

NK cells were conjugated with 221 B-EBV target cells and attached to slides in serum-free RPMI-1640 at 37°C for 15 minutes and stained as previously described.<sup>47</sup> Primary mouse monoclonal antibodies anti-perforin ( $\delta$ G9; BD Biosciences, Oxford, United Kingdom) and antitubulin (TAT-1; a gift from Keith Gull, Sir William Dunn School of Pathology, Oxford University, United Kingdom), or rabbit antiserum against cathepsin D (Upstate, Lake Placid, NY) and either FITC- or Cy3-labeled secondary antibodies (Jackson ImmunoResearch) were used. Samples were analyzed using a Zeiss Axioplan 2 microscope (Carl Zeiss, Hertfordshire, United Kingdom) equipped with a Zeiss Plan-NEOFLUAR 100 $\times$ /1.30 objective lens and mounted with a CoolSnap HQ Camera (Roper Scientific, Tucson, AZ). Images were processed using Metamorph software (Molecular Devices, Downington, PA) and AutoDeblur + AutoVisualize software (AutoQuant Imaging, Watervliet, NY).

## Results

### Perforin and Munc13-4 expression in FHL NK cells

Five patients, identified by FACS analysis as perforin-deficient and confirmed by genetic analysis to carry nonsense perforin mutations (FHL2 subtype), were included in this study (Table 1). Figure 1 shows the FACS profiles of perforin from a representative patient with FHL2 (UPN 314; Figure 1C) in comparison to a healthy control subject (Figure 1A) and a patient with FHL3 (UPN 336; Figure 1B).

Genetic analysis of *MUNC13-4* identified 8 patients with FHL3 with mutations illustrated in Table 2. Figure 2 shows the analysis of Munc13-4 expression in activated polyclonal NK-cell populations derived from 2 healthy donors (H1 and H2), 4 patients with FHL3 (UPNs 237, 336, 293, and 180) and a representative patient with FHL2 (UPN 314). Although equal levels of Munc13-4 are expressed in healthy donors and the patient with FHL2, protein expression is not detected in UPNs 336 and 180, reduced protein levels are detectable in UPN 293, in which the predicted protein possesses a 4 amino acid deletion, and only a trace amount of protein is detected in UPN 237. These results show that the mutations summarized in Table 2 result in greatly reduced or complete loss of Munc13-4 protein expression in NK cells.

### Confocal microscopy analysis of cytotoxic granules in perforin and Munc13-4-defective NK cells

To analyze the perforin localization as well as the polarization of lytic granules in patient or donor NK cells, granules were labeled

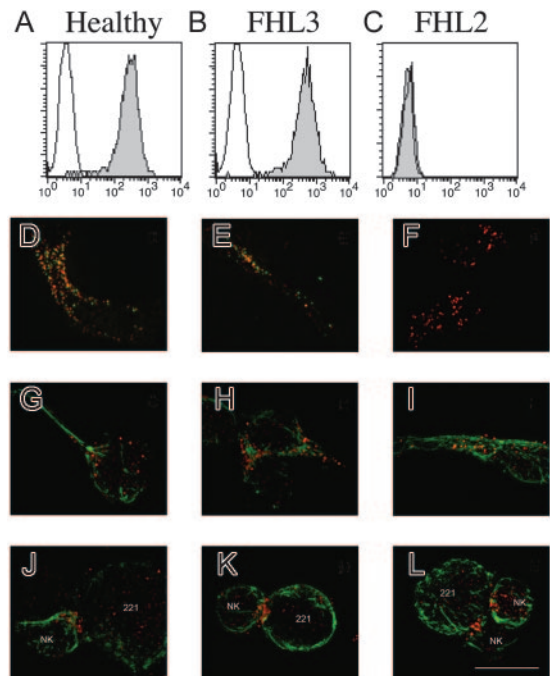


**Figure 1. Perforin expression and granule polarization of patients with FHL compared with control subjects.** Polyclonal activated NK cells derived from healthy donor (A,D,G,J) and patients with FHL3 (UPN 336; B,E,H,K) and with FHL2 (UPN 314; C,F,I,L) were analyzed by flow cytometry (A-C) and confocal microscopy (D-L). Filled curves indicate perforin expression, whereas open curves indicate isotypic control (A-C). Confocal staining of perforin (green) and cathepsin D (red) (D-F) or cathepsin D (red) and tubulin (green) (G-L) is analyzed in isolated NK cells (D-I) or conjugates between NK and target 221 (J-L). Bar indicates 10  $\mu$ m.

using antibodies against perforin, cathepsin D, and microtubules using an antibody against tubulin. NK cells were visualized either alone or conjugated to the 221 B-EBV cell line. Perforin and cathepsin D colocalize in the same granules in control subject (Figure 1D) and the patient with FHL3 patient (UPN 336) (Figure 1E), whereas only cathepsin D is detectable in the patient with FHL2 (UPN 314) (Figure 1F), thus confirming the loss of perforin expression revealed by FACS analysis (Figure 1C). Lytic granules are distributed along microtubules in healthy donor and patients with FHL2 and FHL3 (Figure 1G-I) and polarize tightly at the immunologic synapse (Figure 1J-L), consistent with previous results in CTLs.<sup>9</sup>

### Cytotoxic activity of NK lymphocytes in patients with FHL

Cytolytic activity of freshly derived peripheral blood lymphocytes (PBLs) against K562 target cells (usually referred to as NK activity) was preliminarily tested in patients with FHL3 and found to be markedly reduced.<sup>49</sup> To further characterize this functional impairment, purified NK cells were expanded in IL-2. These activated polyclonal NK cells were tested against a variety of target cells by using a standard <sup>51</sup>Cr-release assay (Figure 3). These included the melanoma FO-1 (Figure 3A, left quadrant) and K562 (not shown) tumor cell lines, the 221 (HLA-class I<sup>-</sup>; Figure 3A, right quadrant) and AMALA (HLA-class I<sup>+</sup>, not shown) B-EBV cell lines, and iDCs (Figure 3B). In addition, the Fc $\gamma$ Rc<sup>+</sup> P815 was tested to assess the function of individual activating receptors in redirected killing assay (Figure 3C). NK cells from patients with FHL2 and healthy donors were tested for comparison. NK cells from patients with FHL3 displayed intermediate levels of cytotoxicity with respect to the high efficiency of killing by NK cells from healthy donors and the inability of killing by perforin-deficient NK

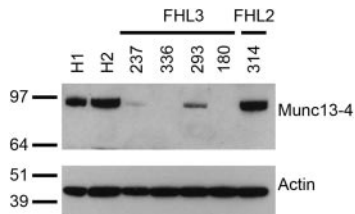


**Figure 2. Munc13-4 expression in control and FHL NK cells.** Cell extracts from polyclonal NK cells of healthy donors (H1, H2), patients with FHL3 (UPNs 237, 336, 293, 180), and patient with FHL2 (UPN 314) were analyzed by Western blot with anti-Munc13-4 antibody. Blots were reprobed with antiactin antibody. Molecular weight standards are shown on the left (kDa).

cells from patients with FHL2. The defect of FHL3 NK cells was more evident against the B-EBV cell lines 221 and AMALA (on mAb-mediated masking of HLA class I) than using the tumor cell lines as target cells. Indeed, killing of K562 was clearly impaired only in patient UPN 336. FO-1 target cells elicited a better discrimination of killing capability and also in this assay UPN 336 appeared the most defective patient. Notably, Munc13-4 expression was completely absent in this patient (Table 2).

Immature DCs, characterized by low surface expression of HLA-class I molecules, are usually highly susceptible to lysis by normal NK cells, in both allogeneic and autologous combination. Indeed, as shown in Figure 3B, NK cells from healthy donors efficiently killed allogeneic iDCs, and lysis was not increased by the addition of anti-HLA class I mAb. Notably, the same iDCs were poorly lysed by the NK cells derived from patients with FHL3, and restoration of lysis was observed on mAb-mediated masking of HLA-class I molecules. Although the values did not reach those of normal NK cells, these data indicate that, because of an inefficient mechanism of lysis induction, the inhibitory receptors can predominate and elicit a strong inhibition of target-cell lysis. As expected, the FHL2 NK cells did not kill even following addition of anti-HLA class I mAb.<sup>50</sup>

We then assessed the ability of different triggering receptors, including NCR, NKG2D, CD16, CD2, and 2B4, to induce killing of P815. In Figure 3C, in UPN 293 strong NK-cell cytotoxicity could be induced by mAbs to NCR (the representative NKp30 is shown), CD16, and NKG2D, although to a lesser extent than NK cells from the healthy control subject. Remarkably, triggering via CD2 and 2B4, that in normal NK deliver a weaker activation signal, were virtually inactive in UPN 293 NK cells. However, in the perforin-deficient NK cells, none of the activation pathways initiated by different receptors resulted in efficient target-cell lysis.

Taken together, these data support the notion that activated NK cells from patients with FHL3 display an impaired cytolytic activity although less marked than in patients with FHL2.

#### CD107a expression in patients with FHL after coculture with target cells

Patients with FHL3 are characterized by critical mutations in the gene encoding Munc13-4, a protein essential for cytolytic granule fusion to the cell surface membrane.<sup>9</sup> Therefore, we further analyzed whether the cell surface expression of CD107a molecule, which marks degranulation in NK cells, was altered.<sup>48,51</sup> Consistent with previous data, resting normal NK cells (CD3<sup>+</sup>CD56<sup>+</sup> gated in PBMCs) were stained with anti-CD107a mAb (range, 5%-25% CD107a<sup>+</sup> cells) when cocultured with K562 (not shown). The percentage of CD107a<sup>+</sup> cells increased when they were incubated overnight with IL-2 before

addition of target cells (range, 27%-75% CD107a<sup>+</sup> cells). To allow an optimal discrimination between normal and pathologic samples, we standardized the assay using a short-term IL-2 cell culture. As shown in Figure 4A, NK cells from a representative healthy individual were compared with those from patients with FHL2 (UPN 314) and 2 different patients with FHL3 (UPNs 293 and 336). Although normal NK cells displayed 73% CD107a<sup>+</sup> cells, NK cells with Munc13-4 defect had only 8% CD107a<sup>+</sup> cells with a dim staining. In contrast, perforin-deficient NK cells, although unable to lyse K562 target cells, showed a very high proportion (41%) of CD107a<sup>+</sup> cells. In Figure 4 (panels B-D), CD107a expression in NK cells from the same donors was also tested using purified polyclonal NK-cell populations. These were incubated with different target cells, such as FO-1 (Figure 4B), K562 (not shown), 221 (Figure 4C), and P815 (redirected killing assay using anti-NKp30 mAb; Figure 4D). The highly susceptible FO-1 and K562 tumor cell lines induced a strong CD107a expression in both healthy and perforin-deficient NK cells (consistently greater than 40%), whereas in Munc13-4-deficient NK cells CD107a expression was lower in terms of both percentage of positive cells and mean fluorescence intensity (MFI; 7 compared with 75 of the healthy donor and 52 of the patient with FHL2). Although the B-EBV cell line 221 was less efficient in inducing CD107a expression by NK cells, differences between healthy and perforin-deficient NK cells as compared with Munc13-4-deficient NK cells were still clearly detectable (11% versus 2%). Finally, when NK cells from healthy individuals were tested against P815 on addition of mAb specific for various activating receptors, similar data (~ 50% CD107a<sup>+</sup> cells) were obtained with NKp30, NKp46, NKp44, and CD16 (results of NKp30 triggering are shown in Figure 4D); in controls, in which no mAb was added, CD107a<sup>+</sup> cells

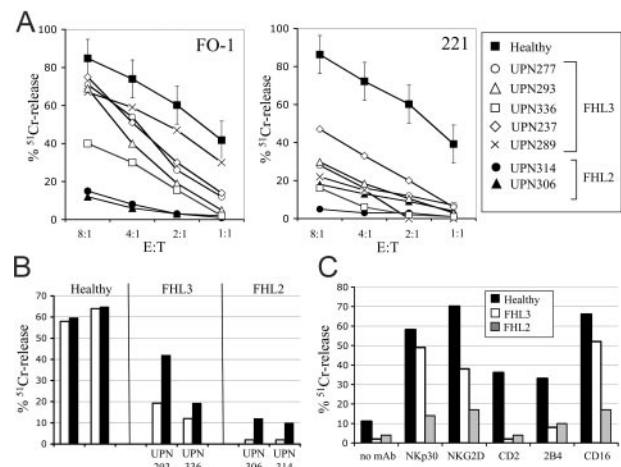


**Figure 3. Cytotoxic activity in patients with FHL.** Using the standard <sup>51</sup>Cr-release assay, polyclonal-activated NK cells derived from patients with FHL3 and FHL2 were compared with those from age-matched healthy individuals for cytolytic activity against various target cells. (A) NK cells from a large group of healthy donors (mean of values, ■, error bars showing ± SD), from 5 different patients with FHL3 (open symbols and crosses) and 2 different patients with FHL2 (● and ▼) were tested against the melanoma FO-1 and the B-EBV cell line 221 at different E/T ratios, as indicated. (B) NK cells from 2 representative healthy individuals and patients with FHL3 and FHL2 were tested against iDCs derived from a single allogeneic healthy individual either in the absence (□) or in the presence (■) of anti-HLA class I mAb. The E/T ratio used was 10:1. (C) NK cells from 1 representative healthy individual and 1 patient with FHL3 (UPN 293), and 1 patient with FHL2 (UPN 314) were tested against the Fcγ-Rc<sup>+</sup> P815 in the absence or in the presence of mAb to different triggering receptors, as indicated. The E/T ratio used was 4:1. Error bars indicate standard error of the mean.

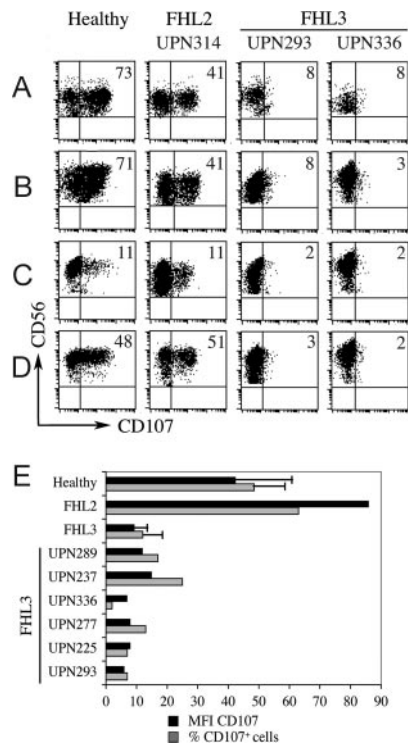


**Figure 4. CD107a surface expression on NK cells, on target interaction, identifies the Munc13-4 defect.** (A) PBMCs from a representative healthy donor, a patient with FHL2 (UPN 314), and 2 patients with FHL3 (UPNs 293 and 336) were cultured overnight in the presence of IL-2 and then cocultured with K562. (B-D) Polyclonal-activated NK-cell populations derived from the same donors were cocultured with FO-1 (B), 221 (C), and P815 with anti-NKp30 (D) mAbs. Cells were stained with anti-CD56-PC5 mAb and anti-CD107a-PE mAb and then analyzed by double fluorescence gating on CD56<sup>+</sup> cells. Numbers indicate the percentage of CD107a<sup>+</sup> cells. In panel E, histograms refer to the percentage of CD107a<sup>+</sup> cells (□) and to the mean fluorescence intensity (MFI) of CD107a surface expression (■) considering CD56<sup>+</sup> cells in a group of patients with FHL3 (mean of 6 ± SD) compared with healthy individuals (mean of 9 ± SD) and patients with FHL2 (mean of 3) after coculture with susceptible target cells. In patients with FHL3, both percentage and MFI were significantly lower than in healthy controls ( $P < .001$ ; Student *t* test). Patients with FHL3 are also shown individually.

were less than 4%. Thus, in normal NK cells the cytofluorimetric analysis using CD107a correlates well with the results of the <sup>51</sup>Cr-release assay (see also Figure 3C). Also in this case, perforin-deficient NK cells displayed normal levels of CD107a expression, whereas FHL3 NK cells were clearly defective. Figure 4E further documents that the defect of CD107a expression (on exposure to various target cells) is a common feature to all patients with FHL3, analyzed as a group as well as individually. In particular CD107a expression was observed in 11.8% ± 7.5% of cells in 6 patients with FHL3, whereas it was 48.5% ± 11.5% in 9 healthy individuals ( $P < .001$ ). The MFI was also significantly lower in the patients with FHL3 compared with the controls (9.3 ± 3.1 versus 42.6 ± 21.9;  $P < .001$ ). In contrast to FHL3, the mean values of CD107a expression obtained from 3 patients with FHL2 were even higher than healthy control subjects in terms of both percentage (63.3%) and MFI (86.6).

Altogether, these data obtained by flow cytometry show that the pattern of CD107a expression represents a novel tool to identify, among patients with FHL, the defect of degranulation which is characteristic of Munc13-4 deficiency. Importantly, in FHL2 NK cells, whose granules lack perforin, the degranulation pattern is normal.

### Cytokine production from NK cells in patients with FHL

Polyclonal NK-cell populations derived from 4 patients with FHL3 and 4 patients with FHL2 were examined for cytokine production and compared with healthy donors. TNF-α (Figure 5) and IFN-γ (not shown) production was induced by NK-cell triggering via anti-NKp30 mAb (Figure 5A) or by overnight coculture with 221 B-EBV cell line (Figure 5B). NKp30 stimulation induced the production of high amounts of both cytokines with no substantial differences between patients and healthy donors. Similar data were obtained on cell stimulation via NKp46, NKp44, and CD16 (not shown). The basal cytokine production (ie, NK cells incubated with no mAb or with anti-CD56 mAb) was similarly low in patients and healthy individuals. However, when NK cells were cultured with 221 cells, a clear difference existed between patients, characterized by high production, and healthy controls, characterized by low production. This difference could be explained by the fact that, in contrast to normal NK cells, those from patients with FHL are inefficient in killing the B-EBV cells (see Figure 3A), which therefore remain alive and continue to provide a stimulatory signal to NK cells. Normal NK cells, efficiently killing 221, rapidly eliminate the source of stimulating interactions. That this might be a likely explanation is further supported by the finding that target cells which are partially lysed by FHL3, such as FO-1 and P815 in the presence of anti-NKp30 mAb (not shown), induced in FHL3 NK-cell cytokine production only slightly above normal cells. In addition NK cells from patients with FHL2 that do not lyse any of the target cells analyzed, consistently produced high amounts of TNF-α when cocultured with these targets.

### Discussion

The present study focuses on the NK-cell function in patients with different FHL subgroups. We show that, by using appropriate target

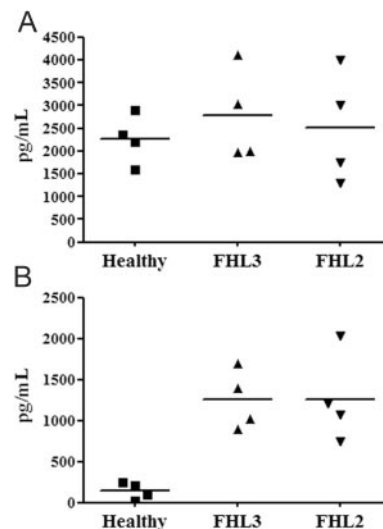


**Figure 5. TNF-α production by patients with FHL compared with healthy donors.** Polyclonal NK-cell populations from 4 different healthy donors, patients with FHL3 (UPNs 249, 237, 225, and 289), and patients with FHL2 (UPNs 210, 235, 256, and 314) were stimulated overnight by plastic-bound anti-NKp30 mAb (A) or by coculture with 221 cell line (B). Supernatants were harvested and analyzed by specific ELISA for their TNFα content. Bars represent the mean of values within a group. Differences among groups were not significant in panel A ( $P > .05$ ), whereas both FHL3 and FHL2 were different ( $P < .05$ ) from the healthy group in panel B (Kruskal-Wallis test).

cells, it is possible to detect both perforin and Munc13-4 defects. Remarkably, we first report that the analysis of CD107a, a marker of granule exocytosis (expressed at the surface of NK cells after their interaction with suitable target cells), in combination with the detection of intracytoplasmic perforin, allows a rapid discrimination between FHL2 and FHL3.

For most patients with FHL, viral infection may represent a serious challenge sometimes difficult to overcome. During viral infection, the balance between the virus and the host may vary and result in different scenarios. When the cytotoxic response is rapid and efficient, infected cells are rapidly killed, and the infection is terminated as a result of the clearance of the virus. If the killing mechanism is inefficient, as in the case of patients with FHL, both T and NK cells become activated and undergo proliferation; however, they fail to kill infected cells and do not arrest virus dissemination. However, because the source of antigen stimulation is not removed, a persistent T-cell and NK-cell activation occurs and results in the production of large amounts of cytokines, including IFN- $\gamma$ , granulocyte-macrophage colony-stimulating factor (GM-CSF) (ie, major macrophage activators), and TNF $\alpha$ . In turn, the macrophage homing to the sites of T-cell and NK-cell triggering and activation results in tissue infiltration and in the production of high levels of primary inflammatory cytokines, including TNF $\alpha$ , IL-1, and IL-6, which play a major role in tissue damage and in the various clinical symptoms. It is of note that HLH represents a clinical syndrome, resulting from inefficient cytolytic function and macrophage hyperactivation, which may be common not only to FHL subtypes but also to different congenital immune defects (including Chédiak-Higashi and Griscelli syndromes). However, a different pathogenic mechanism occurs in male children with X-linked lymphoproliferative disease (XLP), a condition which, in some situations, may be barely distinguishable from HLH.<sup>20,52</sup> Thus, patients with XLP are unable to control Epstein-Barr virus (EBV) infection as a consequence of a major dysfunction of 2B4 receptor which exerts inhibitory instead of activating function.<sup>53</sup> Remarkably, our present data provide a simple *in vitro* model which mimics the effect of the inability of effector cells to clear the source of (antigen) stimulation. Thus, NK cells from healthy individuals, when cocultured with the B-EBV cell line 221, released small amounts of cytokines, whereas those isolated from patients with FHL2 and FHL3 were consistently high producers. The explanation for this difference is that normal NK cells, but not FHL NK cells, rapidly killed target cells, thus removing the source of NK-cell stimulation. Notably, 221 target cells were largely viable after 24 hours of coculture with FHL NK cells. Remarkably, in patients with FHL the overwhelming activation of the immune

system may also result from the marked impairment of NK-mediated killing of iDCs (see Figure 3B and Vitale et al<sup>50</sup>). Indeed, the lack of an efficient DC editing may further lead to an excessive T-cell activation and cytokine release. It should be stressed that potential target cells for NK-mediated lysis *in vivo* are likely to be mostly represented by virus-infected cells and iDCs. Therefore, the insight into NK-cell function provided by our present study may be more representative of the pathophysiology of HLH.

Activated NK cells derived from various patients with FHL3 showed a variable degree of cytotoxic activity against highly susceptible tumor targets. This correlated with the amounts of Munc13-4 protein detected by Western blot analysis. Our results show that even trace amounts of Munc13-4 protein, associated with certain mutations, were sufficient to allow some killing, whereas the complete absence (eg, UPN 336) led to a marked cytolytic defect. FHL2 NK cells were unable to lyse any target, including the highly susceptible ones.

In addition to providing information useful for the pathophysiology of FHL and for a functional correlation with the different mutations, our data may impact on the diagnosis of this disease. Indeed, we report the first use of surface CD107a expression as a novel screening tool for identification, among patients with FHL, those with Munc13-4 defect (FHL3). It is conceivable that other diseases characterized by defects in granule exocytosis may display the same CD107a defective pattern. However, these diseases (eg, Griscelli or Chédiak-Higashi syndromes) can be distinguished from FHL on a clinical ground. On coculture with target cells, NK lymphocytes from patients with FHL3 showed a sharply lower frequency and MFI of CD107a staining compared with healthy control subjects. Thus, the defect of granule exocytosis could be clearly detected. Differently, FHL2 NK cells, lacking perforin in their granules, showed a normal pattern of CD107a staining. Although the use of purified activated NK-cell populations may increase the discrimination power of this test, it is remarkable that even PBMCs (IL-2 activated for 24 hours) could be used to reveal a defect of granule exocytosis. Thus, the combined use of surface expression of CD107a, together with intracytoplasmic staining with anti-perforin mAb,<sup>44</sup> allows to promptly dissect FHL3 and FHL2 defects by the simple analysis of PBMCs, so directing further genetic analysis.

## Acknowledgment

The European Commission is not liable for any use that may be made of the information contained.

## References

- Farquhar J, Claireaux A. Familial haemophagocytic reticulosis. *Arch Dis Child*. 1952;27:519-525.
- Henter JL, Horne AC, Aricò M, et al. Diagnostic and Therapeutic Guidelines for Hemophagocytic Lymphohistiocytosis. *Ped Blood Cancer*. In press.
- Aricò M, Janka G, Fischer A, et al. Hemophagocytic lymphohistiocytosis. Report of 122 children from the International Registry. FHL Study Group of the Histiocyte Society. *Leukemia*. 1996;10:197-203.
- Imashuku S, Hibi S, Sako M, et al. Heterogeneity of immune markers in hemophagocytic lymphohistiocytosis: comparative study of 9 familial and 14 familial inheritance-unproved cases. *J Pediatr Hematol Oncol*. 1998;20:207-214.
- Kanda Y, Tanaka Y, Shirakawa K, et al. Increased soluble Fas-ligand in sera of bone marrow transplant recipients with acute graft-versus-host disease. *Bone Marrow Transplant*. 1998;22:751-754.
- Schneider EM, Lorenz I, Muller-Rosenberger M, et al. Hemophagocytic lymphohistiocytosis is associated with deficiencies of cellular cytolysis but normal expression of transcripts relevant to killer-cell-induced apoptosis. *Blood*. 2002;100:2891-2898.
- Janka G, Imashuku S, Elinder G, Schneider M, Henter JL. Infection- and malignancy-associated hemophagocytic syndromes. Secondary hemophagocytic lymphohistiocytosis. *Hematol Oncol Clin North Am*. 1998;12:435-444.
- Stapp SE, Dufourcq-Lagelouse R, Le Deist F, et al. Perforin gene defects in familial hemophagocytic lymphohistiocytosis. *Science*. 1999;286:1957-1959.
- Feldmann J, Callebaut I, Raposo G, et al. Munc13-4 is essential for cytolytic granules fusion and is mutated in a form of familial hemophagocytic lymphohistiocytosis (FHL3). *Cell*. 2003;115:461-473.
- Ishii E, Ueda I, Shirakawa R, et al. Genetic subtypes of familial hemophagocytic lymphohistiocytosis: correlations with clinical features and cytotoxic T lymphocyte/natural killer cell functions. *Blood*. 2005;105:3442-3448.
- Zur Stadt U, Schmidt S, Kasper B, et al. Linkage of familial hemophagocytic lymphohistiocytosis (FHL) type-4 to chromosome 6q24 and identification of mutations in syntaxin 11. *Hum Mol Genet*. 2005;14:827-834.
- Uellner R, Zvelebil MJ, Hopkins J, et al. Perforin is activated by a proteolytic cleavage during biosynthesis which reveals a phospholipid-binding C2 domain. *EMBO J*. 1997;16:7287-7296.

13. Lowin B, Peitsch MC, Tschopp J. Perforin and granzymes: crucial effector molecules in cytolytic T lymphocyte and natural killer cell-mediated cytotoxicity. *Curr Top Microbiol Immunol.* 1995;198:1-24.
14. Trambas CM, Griffiths GM. Delivering the kiss of death. *Nat Immunol.* 2003;4:399-403.
15. Trapani JA, Smyth MJ. Functional significance of the perforin/granzyme cell death pathway. *Nat Rev Immunol.* 2002;2:735-747.
16. Darmon AJ, Nicholson DW, Bleackley RC. Activation of the apoptotic protease CPP32 by cytotoxic T-cell-derived granzyme B. *Nature.* 1995;377:446-448.
17. Neeft M, Wieffer M, de Jong AS, et al. Munc13-4 is an effector of Rab27a and controls secretion of lysosomes in hematopoietic cells. *Mol Biol Cell* 2005;16:731-741.
18. Shirakawa R, Higashi T, Tabuchi A, et al. Munc13-4 is a GTP-Rab27-binding protein regulating dense core granule secretion in platelets. *J Biol Chem.* 2004; 279:10730-10737.
19. Ménasché G, Pastural E, Feldmann J, et al. Mutations in RAB27A cause Grisel syndrome associated with hemophagocytic syndrome. *Nat Genet.* 2000;25:173-176.
20. Arico M, Danesino C, Pende D, Moretta L. Pathogenesis of hemophagocytic lymphohistiocytosis. *Br J Haematol* 2001;114:761-769.
21. Zamai L, Ahmad M, Bennet IM, et al. Natural killer (NK) cell-mediated cytotoxicity: differential use of TRAIL and Fas ligand by immature and mature primary human NK cells. *J Exp Med.* 1998;188:2375-2380.
22. Screpanti V, Wallin RP, Grandien A, Ljunggren HG. Impact of FASL-induced apoptosis in the elimination of tumor cells by NK cells. *Mol Immunol.* 2005; 42:495-499.
23. Lanier LL. NK cell receptors. *Annu Rev Immunol.* 1998;16:359-393.
24. Moretta A, Bottino C, Mingari MC, Biassoni R, Moretta L. What is a natural killer cell? *Nat Immunol.* 2002;3:6-8.
25. Moretta L, Moretta A. Unravelling natural killer cell function: triggering and inhibitory human NK receptors. *EMBO J.* 2004;23:255-259.
26. Moretta L, Bottino C, Pende D, Vitale M, Mingari MC, Moretta A. Different checkpoints in human NK-cell activation. *Trends Immunol.* 2004;25:670-676.
27. Moretta A, Bottino C, Vitale M, et al. Activating receptors and coreceptors involved in human natural killer cell-mediated cytotoxicity. *Annu Rev Immunol.* 2001;19:197-223.
28. Wu J, Song Y, Bakker ABH, et al. An activating immunoreceptor complex formed by NKG2D and DAP 10. *Science.* 1999;285:730-732.
29. Pende D, Rivera P, Marcenaro S, et al. Major histocompatibility complex class I-related chain A and UL16-binding protein expression on tumor cell lines of different histotypes: analysis of tumor susceptibility to NKG2D-dependent natural killer cell cytotoxicity. *Cancer Res.* 2002;62:6178-6186.
30. Bottino C, Castriconi R, Pende D, et al. Identification of PV9 (CD155) and Nectin-2 (CD112) as cell surface ligands for the human DNAM-1 (CD226) activating molecule. *J Exp Med.* 2003; 198:557-567.
31. Moretta A, Bottino C, Vitale M, et al. Receptors for HLA-class I molecules in human natural killer cells. *Annu Rev Immunol.* 1996;14:619-648.
32. Long EO. Regulation of immune responses through inhibitory receptors. *Annu Rev Immunol.* 1998;17:875-904.
33. Vilches C, Parham P. KIR: diverse, rapidly evolving receptors of innate and adaptive immunity. *Annu Rev Immunol.* 2002;20:217-251.
34. Braud VM, Allan DS, O'Callaghan CA, et al. HLA-E binds to natural killer cell receptors CD94/NKG2A, B and C. *Nature.* 1998;391:795-799.
35. Bottino C, Moretta L, Pende D, Vitale M, Moretta A. Learning how to discriminate between friends and enemies, a lesson from natural killer cells. *Mol Immunol.* 2004;41:569-575.
36. Della Chiesa M, Vitale M, Carlomagno S, et al. The natural killer cell-mediated killing of autologous dendritic cells is confined to a cell subset expressing CD94/NKG2A, but lacking inhibitory killer Ig-like receptors [published correction appears in *Eur J Immunol.* 2003;33:2947]. *Eur J Immunol.* 2003;33:1657-1666.
37. Moretta A. Natural killer cells and dendritic cells: rendezvous in abused tissues. *Nat Rev Immunol.* 2002;2:957-965.
38. Cooper MA, Fehniger TA, Fuchs A, Colonna M, Caligiuri, MA. NK cell and DC interactions. *Trends Immunol.* 2004;25:47-2552.
39. Della Chiesa M, Sivori S, Castriconi R, Marcenaro E, Moretta A. Pathogen-induced private conversations between natural killer and dendritic cells. *Trends Microbiol.* 2005;13:128-136.
40. Moretta A. The dialogue between human natural killer cells and dendritic cells. *Curr Opin Immunol.* 2005;17:306-311.
41. Moretta L, Bottino C, Pende D, et al. Natural killer cells: their origin, receptors and functional role in immune responses. *Eur J Immunol.* 2002;32:1205-1211.
42. Corner BG, Smith HR, French AR, et al. Coordinated expression of cytokines and chemokines by NK cells during murine cytomegalovirus infection. *J Immunol.* 2004;172:3119-3131.
43. Arico M, Allen M, Brusa S, et al. Haemophagocytic lymphohistiocytosis: proposal of a diagnostic algorithm based on perforin expression. *Br J Haematol.* 2002;119:180-188.
44. Kogawa K, Lee SM, Villanueva J, et al. Perforin expression in cytotoxic lymphocytes from patients with hemophagocytic lymphohistiocytosis and their family members. *Blood.* 2002;99:61-66.
45. Henter JL, Samuelsson-Horne A, Arico M, et al. Histocyte Society. Treatment of hemophagocytic lymphohistiocytosis with HLH-94 immunochemotherapy and bone marrow transplantation. *Blood.* 2002;100:2367-2373.
46. Pende D, Parolini S, Pessino A, et al. Identification and molecular characterization of NKp30, a novel triggering receptor involved in natural cytotoxicity mediated by human natural killer cells. *J Exp Med.* 1999;190:1505-1516.
47. Trambas C, Gallo F, Pende D, et al. A single acid change, A91V, leads to conformational changes that can impair processing to the active form of perforin. *Blood.* 2005;106:932-937.
48. Penack O, Gentilini C, Fischer L, et al. CD56dimCD16neg cells are responsible for natural cytotoxicity against tumor targets. *Leukemia.* 2005;19:835-840.
49. Santoro A, Cannella S, Bossi G, et al. Novel Munc13-4 mutations in children and young adult patients with hemophagocytic lymphohistiocytosis. *J Med Genet.* 2006 Jul 6; Epub ahead of print.
50. Vitale M, Della Chiesa M, Carlomagno S, et al. NK-dependent maturation is mediated by TNF $\alpha$  and IFN $\gamma$  released upon engagement of the NKp30 triggering receptor. *Blood.* 2005;106:566-571.
51. Bryceson YT, March ME, Barber DF, Ljunggren HG, Long EO. Cytolytic granule polarization and degranulation controlled by different receptors in resting NK cells. *J Exp Med.* 2005;202:1001-1012.
52. Dupré L, Andolfi G, Tangye SG, et al. SAP controls the cytolytic activity of CD8 $^{+}$  T cells against EBV-infected cells. *Blood.* 2005;105:4383-4389.
53. Parolini S, Bottino C, Falco M, et al. X-linked lymphoproliferative disease. 2B4 molecules displaying inhibitory rather than activating function are responsible for the inability of natural killer cells to kill Epstein-Barr virus-infected cells. *J Exp Med.* 2000;192:337-346.





**blood**<sup>®</sup>

2006 108: 2316-2323  
doi:10.1182/blood-2006-04-015693 originally published  
online June 15, 2006

## **Analysis of natural killer–cell function in familial hemophagocytic lymphohistiocytosis (FHL): defective CD107a surface expression heralds Munc13-4 defect and discriminates between genetic subtypes of the disease**

Stefania Marcenaro, Federico Gallo, Stefania Martini, Alessandra Santoro, Gillian M. Griffiths, Maurizio Aricó, Lorenzo Moretta and Daniela Pende

---

Updated information and services can be found at:  
<http://www.bloodjournal.org/content/108/7/2316.full.html>

Articles on similar topics can be found in the following Blood collections  
[Clinical Trials and Observations](#) (4600 articles)  
[Immunobiology and Immunotherapy](#) (5504 articles)

---

Information about reproducing this article in parts or in its entirety may be found online at:  
[http://www.bloodjournal.org/site/misc/rights.xhtml#repub\\_requests](http://www.bloodjournal.org/site/misc/rights.xhtml#repub_requests)

Information about ordering reprints may be found online at:  
<http://www.bloodjournal.org/site/misc/rights.xhtml#reprints>

Information about subscriptions and ASH membership may be found online at:  
<http://www.bloodjournal.org/site/subscriptions/index.xhtml>